Dissociative Mechanism of Thermal Denaturation of Rabbit Skeletal Muscle Glycogen Phosphorylase *b*†

Boris I. Kurganov,‡ Boris A. Kornilaev,‡ Natalia A. Chebotareva,‡ Vyacheslav Ph. Malikov,*,‡ Victor N. Orlov,§ Arkadii E. Lyubarev,‡ and Natalia B. Livanova‡

A.N. Bach Institute of Biochemistry, Russian Academy of Sciences, Leninsky prospekt 33, Moscow 117071, Russian Federation, and Belozersky Institute of Physico-Chemical Biology, Lomonosov Moscow State University, Moscow 119899, Russian Federation

Received April 27, 2000; Revised Manuscript Received August 8, 2000

ABSTRACT: The thermal stability of rabbit skeletal muscle glycogen phosphorylase *b* was characterized using enzymological inactivation studies, differential scanning calorimetry, and analytical ultracentrifugation. The results suggest that denaturation proceeds by the dissociative mechanism, i.e., it includes the step of reversible dissociation of the active dimer into inactive monomers and the following step of irreversible denaturation of the monomer. It was shown that glucose 1-phosphate (substrate), glucose (competitive inhibitor), AMP (allosteric activator), FMN, and glucose 6-phosphate (allosteric inhibitors) had a protective effect. Calorimetric study demonstrates that the cofactor of glycogen phosphorylase—pyridoxal 5′-phosphate—stabilizes the enzyme molecule. Partial reactivation of glycogen phosphorylase *b* preheated at 53 °C occurs after cooling of the enzyme solution to 30 °C. The fact that the rate of reactivation decreases with dilution of the enzyme solution indicates association of inactive monomers into active dimers during renaturation. The allosteric inhibitor FMN enhances the rate of phosphorylase *b* reactivation.

One of the most important physicochemical characteristics of the proteins is their stability at elevated temperatures. The kinetics of the denaturation of proteins possessing the quaternary structure has certain peculiarities because the overall mechanism of denaturation can include the step of reversible dissociation of the protein oligomer into separate subunits. For oligomeric proteins undergoing denaturation through the dissociative mechanism, the shape of kinetic curves of denaturation varies with variation of the protein concentration. The dissociative mechanism of thermal denaturation has been demonstrated for glyceraldehydes-3-phosphate dehydrogenase from lobster muscle (*1*), β-galactosidase from *Escherichia coli* (*2*) and *Streptococcus thermophilus* (*3*), glucosamine 6-phosphate deaminase from *E. coli* (*4*), glutamate dehydrogenase from *Sulfolobus solfataricus* (*5*) and bovine liver (*6*), β-lactoglobulin (*7, 8*), NAD-kinase from rabbit liver (*9*), aminoacylase I from porcine kidney (*10*), and adenylate kinase from *Sulfolobus acidocaldarius* (*11*).

Glycogen phosphorylase *b* is an excellent object for studying the mechanism of thermal denaturation of oligomeric enzymes, because phosphorylase *b* is a dimeric enzyme with its structure as well as the catalytic and regulatory properties studied in detail. The catalytically active form of the enzyme is a dimer, whereas monomers (*12*) and tetramers (*13*, *14*) are inactive. The dimeric molecule is composed of two identical subunits (97 000 Da) (Figure 1) (*15*). In addition to the active site including pyridoxal phosphate as a cofactor, each subunit also carries a spatially separated allosteric activatory site (for binding of AMP) close to the contact between subunits, and an allosteric inhibitory site inside the subunit globule in the area of the contact of N- and C-domains. The adenine moiety of AMP is sandwiched between the aromatic ring of Tyr-75 (from α-2-helix) and the side chain of Val-45′ (from the cap of the neighboring subunit). Various heterocyclic compounds, including adenine, adenosine, flavins, and caffein, are bound at the inhibitory site. The binding site for glucose 6-phosphate, which acts as an inhibitor, partly overlaps with the site for AMP binding. The glucose ring stacks against the side chain of Trp-67 (the two rings are nearly perpendicular) and the O2 hydroxyl forms a good hydrogen bond with the carbonyl oxygen of Val-40′. Both O1 and O5 are involved in an interaction with Arg-193 (*16*).

The goal of the present work was to study the mechanism of thermal denaturation of glycogen phosphorylase *b* and the influence of specific ligands on this process using the data on thermal inactivation kinetics, analytical ultracentrifugation, and differential scanning calorimetry (DSC).[1] The ability of the enzyme to reactivation was also investigated.

MATERIALS AND METHODS

Materials. Hepes and glucose 1-phosphate were purchased from Sigma, AMP and glucose 6-phosphate from Reanal (Hungary), pig liver glycogen with molecular mass of 5.5

† This work was supported by Grants 99-04-48639, 99-04-49133, and 00-15-97787 from the Russian Foundation for Basic Research.

* To whom correspondence should be addressed. Present address: University of Connecticut Health Center, 263 Farmington Avenue, MC 1507, Farmington, CT, 06032-1507. Phone: (860) 679-4711. Fax: (860) 679-1039. E-mail: malikov@nso.uchc.edu.

‡ A.N. Bach Institute of Biochemistry.

§ Belozersky Institute of Physico-Chemical Biology.

[1] Abbreviation: DSC, differential scanning calorimetry.

10.1021/bi000975w CCC: $19.00
Published on Web 09/29/2000

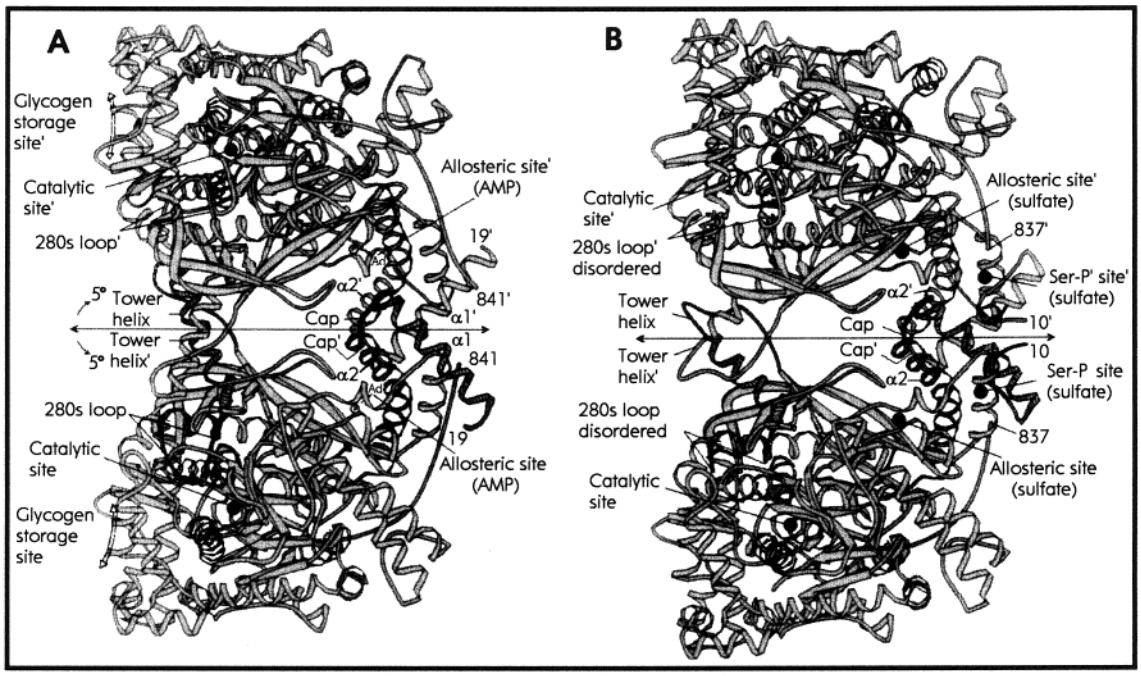

FIGURE 1: Ribbon representation of the structure of T (A) and R (B) states of muscle phosphorylase *b* dimer viewed perpendicular to the molecular dyad axis [Reprinted with permission from Barford, D., and Johnson, L. N. (*15*)].

$\times$ 10^6 Da from Biolar (Latvia), glucose from Reakhim (Russia), and FMN from Scientific-Industrial Association Vitaminy (Russia).

Phosphorylase b Preparation. Phosphorylase *b* was prepared from rabbit skeletal muscle according to the method described by Fisher and Krebs (*17*), using dithiotreitol instead of cysteine. Preparations of the enzyme recrystallized four times and freed of AMP were used in the experiments. Phosphorylase *b* preparations were stored at -20 °C in β-glycerophosphate-NaOH-buffer, pH 6.8, containing 50% glycerol and 0.03 M β-mercaptoethanol. Phosphorylase *b* concentration was determined spectrophotometrically using absorbance index $A^{1\%}$ of 13.2 at 280 nm (*18*).

Phosphorylase b Assay. The activity of phosphorylase *b* in the direction of glycogen synthesis was determined by the turbidimetric method proposed in our paper (*19*). The increase in the optical absorbance of glycogen solution was registered at 360 nm using a Hitachi-557 spectrophotometer (Japan) equipped with a thermostated cell holder with 1-cm optical path length cuvettes. The activity measurements were carried out at 30 °C in 0.08 M Hepes-NaOH buffer, pH 6.8. Phosphorylase *b* concentration in the reaction mixture was 10 μg/mL. To calculate the initial rate of phosphorylase reaction, the linear parts of the kinetic curves were used (for the native enzyme the linearity is retained for 5 min).

Preparation of Apoform and Reduced Form of Phosphorylase b. Apophosphorylase *b* was prepared according to Shaltiel et al. (*20*). Reconstitution of phosphorylase *b* was carried out by addition of equimolar quantities of PLP into the solution of apophosphorylase *b* (*21*). Reduction of phosphorylase *b* by sodium borohydride was carried out according to (*22, 23*).

Thermal Inactivation and Reactivation of Phosphorylase b. To study the kinetics of thermal inactivation of phosphorylase *b* at elevated temperatures (80 mM Hepes-NaOH, pH 6.8), the enzyme solution was placed into the thermostated bath, and temperature was maintained with accuracy ± 0.05 °C. Enzyme aliquots were withdrawn from the solution at fixed intervals. Enzyme activity was determined by the addition of the enzyme solution to the reaction mixture preincubated at 30 °C.

To study the reactivation of phosphorylase *b* preheated at 51 or 53 °C, the enzyme solution was cooled to 30 °C, and then aliquots were withdrawn from the cooled solution at certain time intervals to determine the enzymatic activity.

Analytical Ultracentrifugation. Sedimentation of phosphorylase *b* was studied using an analytical ultracentrifuge Spinco, model E (Beckman), equipped with a photoelectric scanner, a multiplexer, and a monochromator. We used a titanium rotor An-F-Ti and double-sector cells with 12-mm charcoal-filled Epon centerpieces in the sedimentation experiments. The rotor speed was 44000$-$60000 rpm. Scanning was carried out at the wavelengths 290 and 280 nm. The sedimentation velocity studies were performed at 49$-$53 °C (80 mM Hepes-NaOH, pH 6.8). The cell with the enzyme solution was placed into the rotor preheated to the required temperature and optical absorbance was registered after different times of incubation. The first registration was carried out during rotor acceleration at low rotor speed (3000 rpm) after 5-min incubation of the enzyme.

The sedimentation coefficient was normalized to the standard conditions (a solvent with the density and viscosity of water at 20 °C) using the equation

$$s_{20,w} = s_t\left(\frac{\eta_t}{\eta_{20}}\right)\left(\frac{\eta_{sol}}{\eta_w}\right)\left(\frac{1-\bar{v}_{20}\rho_{20,w}}{1-\bar{v}_t\rho_{t,sol}}\right) \quad (1)$$

where s_t is the sedimentation coefficient at the chosen temperature (t), η_t and η_{20} are the viscosity of water at the temperature t and 20 °C, respectively, η_{sol}/η_w is the solvent and water viscosities ratio, $\bar{v}_{20}$ is partial specific volume of enzyme at 20 °C, $\rho_{20,w}$ is water density at 20 °C, $\rho_{t,sol}$ is solvent density at temperature t, $\bar{v}_t$ is partial specific volume

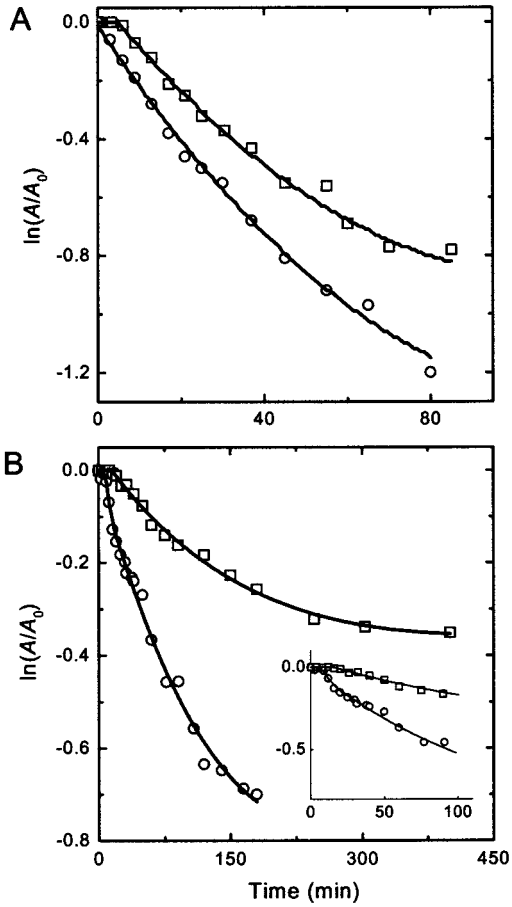

FIGURE 2: Kinetics of thermal inactivation of phosphorylase *b* at 53 °C (A) and 51 °C (B) in semilogarithmic coordinates (80 mM Hepes-NaOH, pH 6.8). A/A_0 is the relative enzymatic activity, *t* is time. Enzyme concentrations are 1.6 mg/mL (circles) and 5.2 mg/mL (squares). Insert in panel B shows the initial parts of the kinetic curves (the axes are identical with those for the main figure).

of enzyme at the temperature *t*, calculated as $\bar{v}_t = \bar{v}_{20} + (d\bar{v}/dt)(t - 20)$, within $(d\bar{v}/dt)$ taken equal to 0.000 36 mL/g deg (*24*).

Calorimetric Studies. Calorimetric measurements were carried out on a differential scanning adiabatic microcalorimeter DASM-4 (NPO "Biopribor", Russian Academy of Sciences) with the capillary platinum cells (an operating volume of 0.47 mL). To obtain the heat capacity curves, the phosphorylase *b* solution in 30 mM Hepes-KOH buffer, pH 7.0, was placed into the cell and heated from 20 to 80 °C with the certain rate (the typical rate was 1 °C/min).

Fitting systems of theoretical equations to DSC data was carried out using the commercial software "Scientist" (MicroMath Scientific Software).

RESULTS

Kinetics of Thermal Inactivation of Glycogen Phosphorylase b. As was shown by us previously (*25*), at the relatively low concentrations of phosphorylase *b* (lower than 0.1 mg/mL), protein denaturation on the surface of the tube contributed substantially to the overall process of denaturation. Therefore, the study of the kinetics of thermal inactivation of phosphorylase *b* was carried out at the enzyme concentrations higher than 1 mg/mL.

Figure 2A shows the curves of thermal inactivation of phosphorylase *b* obtained at various concentrations of the enzyme (53 °C). First, it should be noted that variation in the concentration of phosphorylase *b* causes the change in the rate of enzyme thermal inactivation: it proceeds faster when the enzyme concentration decreases. A similar picture was observed for thermal inactivation of a number of other enzymes (*5*, *26*, *27*) and is generally interpreted as an evidence for the dissociative mechanism of denaturation. This mechanism involves the step of reversible dissociation of the enzyme oligomer into subunits, the latter being essentially more labile than the original oligomer of the enzyme.

Table 1: Effect of Concentration of Phosphorylase *b* (C_t) and the Scanning Rate (v) on the Parameters of DSC Curves (30 mM Hepes-KOH, pH 7.0)

C_t (mg/mL)	v (K/min)	t_m (°C)	$\Delta C_{p,max}$ (kJ mol^{-1} K^{-1})	ΔH_{cal} (kJ/mol)
0.5	0.25	55.5	251	1014
0.5	1	58.3	178	1199
0.5	2	60.1	151	1239
0.3	1	57.9	164	1234
1	1	58.3	180	1350
3	1	58.6	221	1253
6	1	59.0	246	1290

It is also noteworthy that at rather high concentrations of phosphorylase *b*, the lag period is observed on the thermal inactivation curves (Figure 2A; $[E]_0 = 5.2$ mg/mL). The lag period becomes more pronounced as the temperature decreases. As is seen from Figure 2B, at lower temperature, namely at 51 °C, the lag period is well marked both at $[E]_0 = 1.6$ and $[E]_0 = 5.2$ mg/mL. In the framework of the dissociative mechanism of denaturation of oligomeric enzymes, the lag period on the thermoinactivation curves appears because the initial stage of denaturation is a reversible conformational transition of the enzyme oligomer, which proceeds without change in the catalytic properties of the enzyme.

Study of Phosphorylase b Thermal Stability by DSC. Thermal denaturation of phosphorylase *b* was calorimetrically irreversible because no thermal effect was observed at reheating scans. Moreover, the main parameters of DSC curve, namely, the maximum value of the excess heat capacity ($\Delta C_{p,max}$) and temperature corresponding to $\Delta C_{p,max}$ (t_m), were dependent on the scanning rate and protein concentration, as it is demonstrated in Table 1. The fact that t_m is a function of the scanning rate testifies to the kinetic control of denaturation of phosphorylase *b* (*28*). The fact that t_m and $\Delta C_{p,max}$ are the functions of the protein concentration can be explained by the existence of the step of reversible dissociation in the process of thermal denaturation.

Sanchez-Ruiz (*28*) studied theoretically the model of thermal denaturation of an oligomeric protein including the step of reversible dissociation of the protein into monomers and the step of irreversible denaturation of the monomers:

$$E_2 \underset{k_{-1}}{\overset{k_1}{\rightleftharpoons}} 2E_1 \xrightarrow{k_2} 2E_{den} \qquad (2)$$

Assuming that the irreversible step is rate limited ($k_2 \ll k_1, k_{-1}[E_1]$) and the equilibrium at the first step is shifted toward the oligomer ($K = k_1/k_{-1} \ll C_t$; C_t is the total concentration of the protein), Sanchez-Ruiz has showed that t_m on DSC curves is shifted toward higher temperatures with increase in the protein concentration. The results of the

thermal stability studies of glucosamine 6-phosphate deaminase from *E. coli*, which exists as a hexamer in solution (*4*), provide support for this prediction: the shift of the maximum from 57 to 66 °C was observed when the enzyme concentration increased from 0.61 to 7.3 mg/mL.

The data presented in Table 1 and Figure 3 show that an increase in phosphorylase *b* concentration from 0.3 to 6 mg/mL shifts the position of ΔC_p maximum from 57.9 to 59.0 °C. This shift is small in comparison with the theoretical prediction by Sanchez-Ruiz and the case of glucosamine 6-phosphate deaminase. It is of special interest that the increase in phosphorylase *b* concentration results in the significant increase of the $\Delta C_{p,max}$ value.

The assumptions made by Sanchez-Ruiz are not probably valid for thermal denaturation of phosphorylase *b*. Therefore we have used the general case of the model (*2*) where all three rate constants should be taken into account. We assume that these constants change with temperature according to the Arrhenius equation: $k = \exp\{E_a(1/T^* - 1/T)/R\}$ (E_a is the energy of activation, R is the gas constant, and T^* is the absolute temperature at which the rate constant equals 1 min^{-1}).

The kinetic behavior of the system following the model (2) is described by the system of differential equations:

$$\begin{cases} \dfrac{d[E_2]}{dT} = \dfrac{1}{v}\left(k_{-1}\dfrac{[E_1]^2}{2} - k_1[E_2]\right) \\ \dfrac{d[E_1]}{dT} = \dfrac{1}{v}(2k_1[E_2] - k_{-1}[E_1]^2 - k_2[E_1]) \end{cases} \quad (3)$$

where $[E_2]$ and $[E_1]$ are the concentrations of the forms E_2 and E_1, respectively, v is the scanning rate. The excess heat capacity is expressed as

$$\Delta C_p = \frac{\Delta H_1(k_1[E_2] - k_{-1}[E_1]^2/2) + \Delta H_2 k_2[E_1]}{vC_t} \quad (4)$$

where ΔH_1 and ΔH_2 are enthalpies of the first and second steps. The total enthalpy change for protein denaturation is equal to $\Delta H_1 + 2\Delta H_2$.

We have carried out fitting of the system of eqs 3 and 4 simultaneously to three DSC curves obtained at various protein concentrations. Figure 3 shows that two experimental curves (at protein concentration of 3 and 6 mg/mL) coincide very well with the theoretical curves. Some deviations are observed when comparing the third curve (at protein concentration of 0.5 mg/mL) with the theoretical curve. The coefficient of determination characterizing the accuracy of fitting was 0.993. The values of parameters obtained are shown in Table 2.

Thus, the model of dissociative denaturation represented by the kinetic eq 2 allows us to describe satisfactorily the main peculiarities of DSC profiles obtained at various concentrations of phosphorylase *b*: the relatively small shift of t_m and simultaneously rather marked change in the $\Delta C_{p,max}$ value at variation of the enzyme concentration.

Study of Phosphorylase b Dissociation at Elevated Temperature by Sedimentation Velocity Analysis. Figure 4 shows sedimentation patterns obtained at different times after reaching 60 000 rpm at various concentrations of the enzyme. The sedimentation coefficient of the major boundary decreases with decreasing the protein concentration from 7.9 S at $[E]_0 = 2.5$ mg/mL (Figure 4D) to 5.5 S at $[E]_0 = 0.3$ mg/mL (Figure 4A). The sedimentation coefficient, $s_{20,w}$, for the native dimeric form of phosphorylase *b* was estimated to be 8.2 S. As for the monomeric form of phosphorylase *b*, it is known that the sedimentation coefficient for the monomeric form of apoenzyme is equal to 4.9−5.3 S (*29*). The decrease in the sedimentation coefficient for the quickly sedimenting boundary with decreasing the enzyme concentration can be explained assuming a rapid equilibrium between the dimeric and monomeric forms of the enzyme. Actually, in this case both forms sediment as a single boundary with a sedimentation coefficient close to the weight-average value (*30*, *31*). Dilution of the enzyme solution should result in increasing the proportion of the monomeric form and consequently diminishing the sedimentation coefficient value. The slowly sedimenting boundary with $s_{20,w}$ equal to 4.4−5.4 S (Figure 4) probably corresponds to the irreversibly denatured form of the monomer. In addition, the upper parts of the sedimentation velocity profiles (Figure 4, panels A and B) are indicative of the presence of aggregates. Thus, the sedimentation data support the dissociative mechanism of thermal denaturation of phosphorylase *b*.

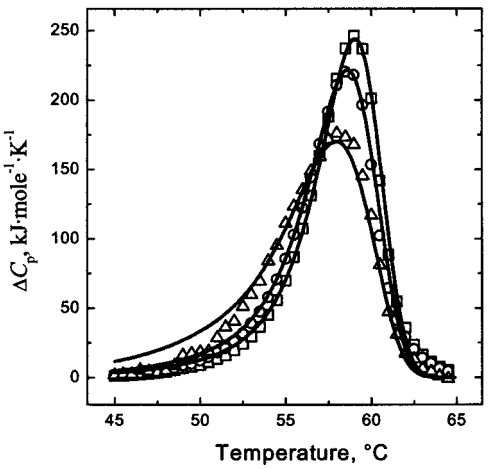

FIGURE 3: Excess heat capacity (ΔC_p) vs temperature profiles for phosphorylase *b*. Enzyme concentrations were: 0.5 mg/mL (triangles), 3.0 mg/mL (circles), and 6.0 mg/mL (squares). Hepes-KOH, 30 mM, pH 7.0. The scanning rate was 1 °C/min. Solid lines are the best fit simultaneously to all the curves based on model (*2*).

Table 2: Parameters of the Dissociative Mechanism of Thermal Denaturation of Phosphorylase *b* Described by the Model (*2*)

parameter	value
ΔH_1 (kJ/mol of dimer)	429 ± 14
ΔH_2 (kJ/mol of monomer)	437 ± 8
$E_{a,1}$ (kJ/mol of dimer)	578 ± 18
$E_{a,-1}$ (kJ/mol of monomer)	149 ± 11
$E_{a,2}$ (kJ/mol of monomer)	373 ± 4
T_1^* (K)	319.8 ± 0.8
T_{-1}^* (K)	249.9 ± 2.9
T_2^* (K)	333.3 ± 0.03

Study of the Reversibility of Thermal Inactivation of Phosphorylase b. The possibility of reactivation of the heated enzyme by subsequent cooling due to reassociation of inactive monomers into active oligomers has been shown for several oligomeric enzymes, e.g., for acid phosphatase

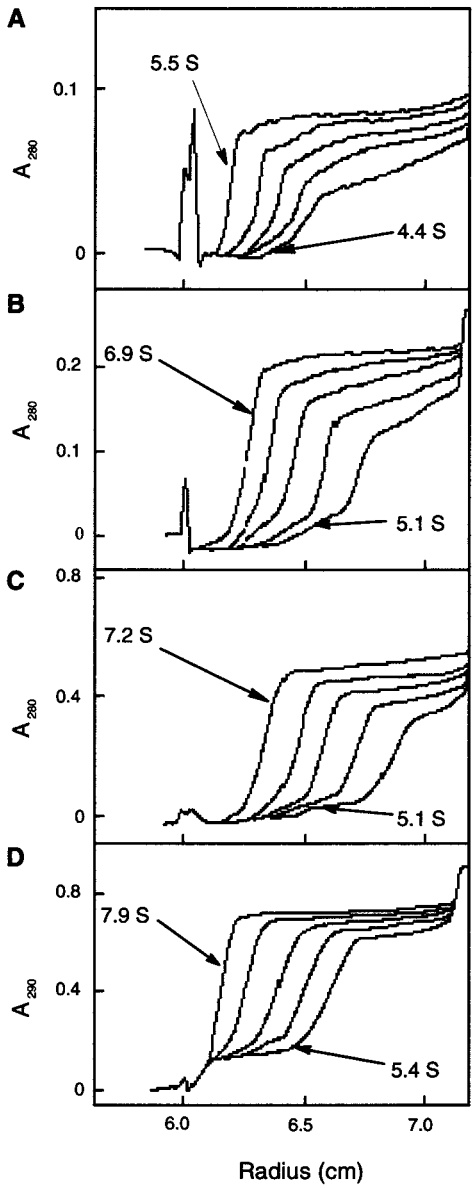

FIGURE 4: Sedimentation of phosphorylase *b* at 53 °C (80 mM Hepes-NaOH, pH 6.8). Enzyme concentration: (A) 0.3; (B) 0.46; (C) 0.92, and (D) 2.5 mg/mL. Time after reaching 60 000 rpm: (A) 6, 14, 20, 25, and 33 min; (B) 10, 15, 21, 27, and 34 min; (C) 12, 18, 23, 29, and 36 min; (D) 7, 13, 18, 22, and 27 min. Ordinate axes show optical density at 280 or 290 nm.

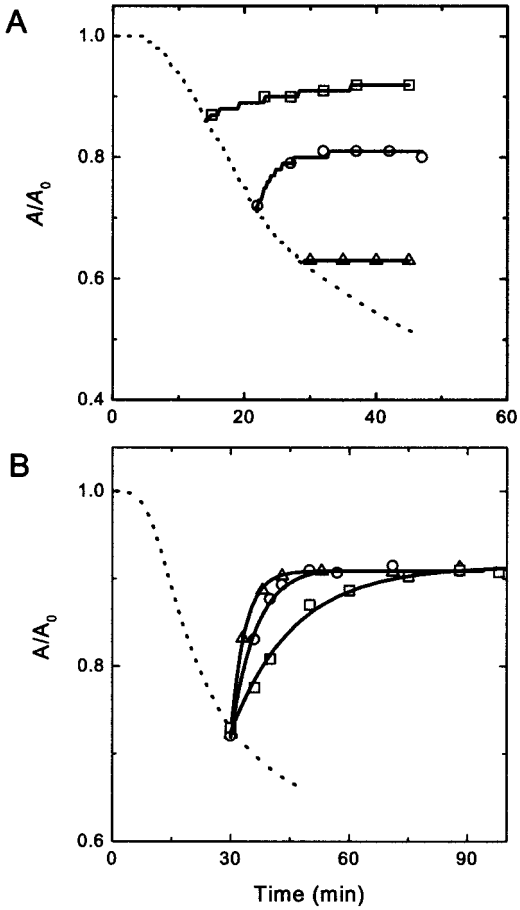

FIGURE 5: Reactivation of phosphorylase *b* after thermal treatment. (A) Kinetics of reactivation of the enzyme preheated at 53 °C for 15 min (squares), 22 min (circles), and 30 min (triangles). Reactivation was studied at 30 °C. The dotted line corresponds to the thermoinactivation curve of phosphorylase *b* at 53 °C. Enzyme concentration was 5.2 mg/mL (80 mM Hepes-NaOH, pH 6.8). (B) Effect of the protein concentration on the kinetics of reactivation of phosphorylase *b* at 30 °C. The enzyme solution (5.2 mg/mL) was preheated at 51 °C for 30 min. Reactivation was carried out at the following enzyme concentrations: 1.3 mg/mL (squares), 2.6 mg/mL (circles), and 5.2 mg/mL (triangles). The dotted line corresponds to the thermal inactivation curve of phosphorylase *b* (5.2 mg/mL) at 51 °C.

from *Aspergillus terreus* (*32*). It was of special interest to study the possibility of reactivation of phosphorylase *b* after heating of the enzyme during different time intervals.

As illustrated in Figure 5A, the enzymatic activity of phosphorylase *b* preincubated at 53 °C during different time intervals is partly recovered after cooling of the solution to 30 °C. For the enzyme preheated for 15 min when its activity decreases to 85% compared to the initial level, the activity is recovered up to 93% after cooling. In the sample preheated for 22 min, the activity after cooling is recovered from 70 to 80%. After heating of the enzyme solution for 30 min, no reactivation is observed. Thus, under these conditions denaturation becomes completely irreversible.

To understand the mechanism of reactivation of phosphorylase *b*, the initial enzyme solution (5.2 mg/mL) was preheated at 51 °C for 30 min and the kinetics of the activity recovery was registered at various enzyme concentrations: 5.2 mg/mL (without dilution), 2.6 (2-fold diluted solution), and 1.3 mg/mL (4-fold diluted solution) (Figure 5B). If reactivation results from reassociation of two inactive monomers into an active dimer, then the rate of the activity recovery should decrease with dilution of phosphorylase *b* solution, because the rate of reassociation of two inactive monomers into an active dimer (as the rate of a bimolecular reaction) is proportional to the square of the monomer concentration. In fact, the dilution results in slowing of the reactivation process. Thus, it is believed that from the kinetic point of view reactivation is mainly determined by irreversible association of monomers into dimer.

Influence of Specific Ligands on Thermodenaturation and Reactivation of Phosphorylase b. Figure 6 shows the effect of specific ligands on the temperature dependence of phosphorylase *b* excess heat capacity (ΔC_p). In the absence of ligands, the excess heat capacity vs temperature curve is asymmetric, with temperature maximum positioned at 56.8 °C. For all the ligands tested, used in the concentrations close to the saturating ones, the temperature maximum of the

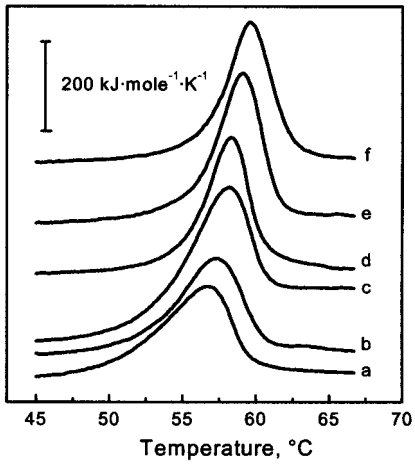

FIGURE 6: Excess heat capacity (ΔC_p) vs temperature profiles for phosphorylase *b* (5.2 mg/mL) obtained in the absence of specific ligands (a) and in the presence of 20 mM glucose 1-phosphate (b), 3 mM AMP (c), 100 mM glucose (d), 10 mM glucose 6-phosphate (e), or 1 mM FMN (f). 30 mM Hepes-KOH, pH 7.0. The scanning rate was 1 °C/min.

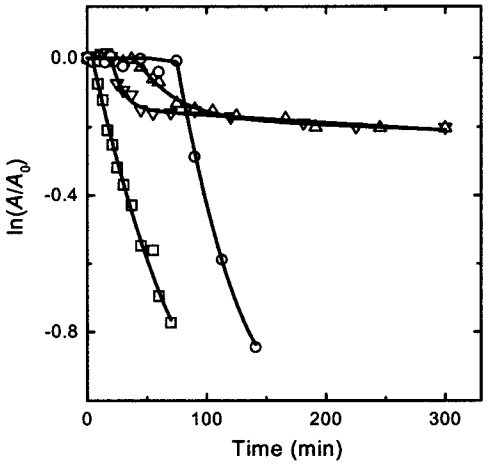

FIGURE 7: Effect of 2 mM FMN (○), 1.8 mM AMP (▽), and 3 mM glucose 6-phosphate (△) on the kinetics of thermal inactivation of phosphorylase *b* (5.2 mg/mL; 53 °C). Squares correspond to thermoinactivation of the enzyme without any additions. The data are presented in semilogarithmic coordinates. Hepes-NaOH, 80 mM, pH 6.8.

curves increases in the following order: 57.4 °C for the substrate glucose 1-phosphate, 58.1 °C for the allosteric activator AMP, 58.3 °C for the competitive inhibitor glucose, 59.1 °C for the allosteric inhibitor glucose 6-phosphate, and 59.6 °C for the allosteric inhibitor FMN. The maximal protective effect was observed for FMN.

It should be noted that the protective effect of AMP is not disturbed by possible formation of tetramer, because the control sedimentation experiments (not illustrated) testify to absence of the tetrameric form at temperatures higher than 45 °C (at the enzyme concentration 5.2 mg/mL).

The character of the thermal inactivation curves at 53 °C in the presence of FMN, AMP, and glucose 6-phosphate is substantially different from that without ligands (Figure 7). As is seen from the figure, the duration of the lag period is markedly increased in the presence of each ligand, i.e., the ligands studied interfere with the reversible predenaturational conformational changes in the dimeric molecule of phosphorylase *b*. The most pronounced effect at this step was

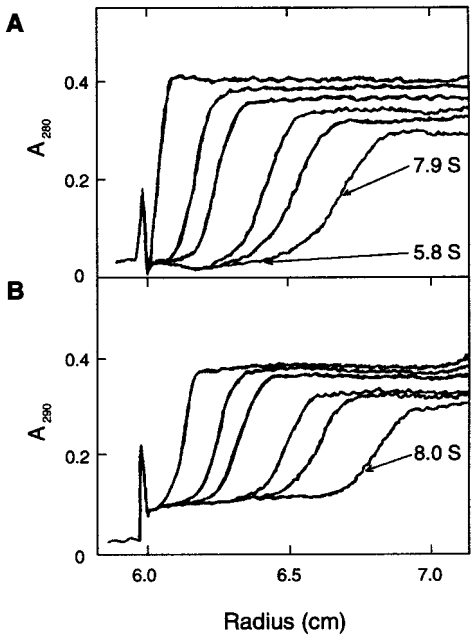

FIGURE 8: Sedimentation velocity patterns of phosphorylase *b* (0.57 mg/mL) at 49 °C in the absence of AMP (A) and in the presence of 1 mM AMP (B). The rotor speed was 48 000 rpm. The times after attaining the maximum speed were 3, 10, 17, 29, 37, and 50 min (A); 6, 14, 22, 32, 41, and 55 min (B).

detected for FMN. Surprisingly, after sufficient length of time ($t > 100$ min) the rate of inactivation in the presence of FMN appears to be substantially higher than that in the presence of AMP or glucose 6-phosphate.

The slow of phosphorylase *b* inactivation at high values of time in the presence of AMP and glucose 6-phosphate is probably due to ability of these ligands to interfere with dissociation of dimer into monomers. This suggestion was supported by the sedimentation experiments. During the sedimentation studies of phosphorylase *b* (0.57 mg/mL) at 49 °C, we observed two boundaries, one of which corresponds to the dimeric form with $s_{20,w} = 7.9$ S and the other which corresponds to the monomeric form with $s_{20,w} = 5.8$ S (Figure 8A). However, only one boundary with $s_{20,w} = 8.0$ S was observed on the sedimentation patterns obtained in the presence of 1 mM AMP (Figure 8B).

Figure 9 shows the effect of specific ligands on reactivation of phosphorylase *b* preheated at 51 °C for 30 min. As can be seen from the figure, the kinetic curve of reactivation obtained in the absence of ligands coincides with that obtained in the presence of AMP or glucose 6-phosphate. This means that AMP and glucose 6-phosphate do not affect the rate of the reactivation process. However, in the presence of 2 mM FMN, a pronounced acceleration of reactivation is observed. It is noteworthy that none of the ligands influenced the maximum degree of the enzymatic activity recovery.

Role of PLP in Stabilization of the Phosphorylase b Molecule. To characterize the role of cofactor of phosphorylase *b*, PLP, in sustaining the native conformation of the enzyme, we carried out a comparative analysis of thermal stability of the native phosphorylase *b* (holoform) and its apoform using DSC. As can be seen from Figure 10, a maximum on the ΔC_p vs temperature profile for the apoform of phosphorylase *b* (48 °C) is shifted markedly toward lower temperatures in comparison with that for the holoform (56.8

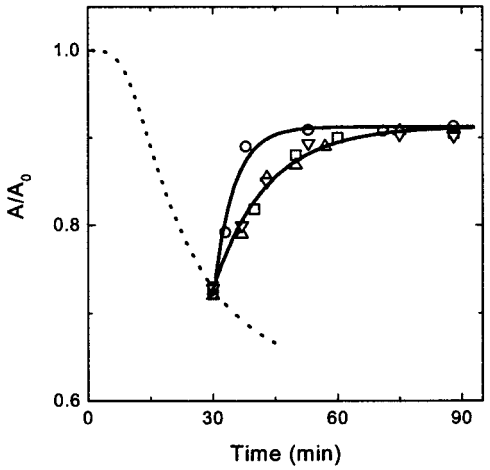

FIGURE 9: Effect of 2 mM FMN (○), 1.8 mM AMP (▽), and 3 mM glucose 6-phosphate (△) on the kinetics of reactivation of phosphorylase *b* (1.3 mg/mL) preheated at 51 °C for 30 min. Squares correspond to reactivation in the absence of ligands. Reactivation was studied at 30 °C. The dotted line is the thermal inactivation curve of phosphorylase *b* (5.2 mg/mL) at 51 °C. When studying reactivation, the preheated enzyme solution was diluted to 1.3 mg/mL.

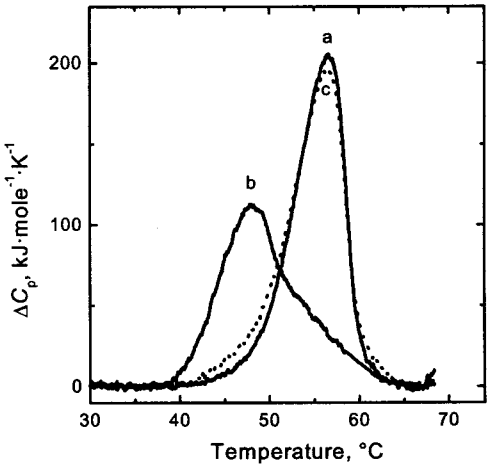

FIGURE 10: Excess heat capacity (ΔC_p) vs temperature profiles for holoform (a), apoform (b), and reconstituted form (c) of phosphorylase *b* (30 mM Hepes-KOH, pH 7.0). Enzyme concentration was 0.7 mg/mL for all the enzyme preparations. The scanning rate was 1 °C/min.

°C). Thermostability of the reconstituted enzyme (curve c) is practically identical to that for the native enzyme. It is known that removal of PLP from phosphorylase *b* results in dissociation of the dimeric form into monomers (*29*, *33*). Therefore, one can assume that the main reason for the lesser stability of the apoform of the enzyme is its being in the monomeric state. Nevertheless, it is evident that PLP has a general stabilizing effect on the conformation of the native phosphorylase *b*.

In the phosphorylase *b* molecule, PLP is bound by aldimine bond with Lys-680. The study of thermal stability of modified phosphorylase *b* where aldimine bond is reduced by sodium borohydride gives an additional verification of participation of PLP in stabilization of the native enzyme molecule. As is seen from Figure 11, thermal inactivation of phosphorylase *b* reduced by sodium borohydride proceeds much faster in comparison with the native enzyme. The following two circumstances are worth mentioning. First, the

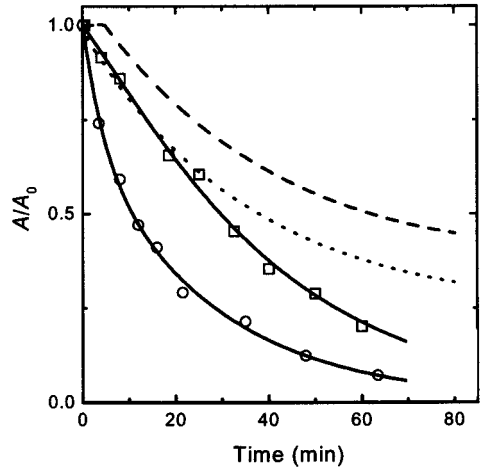

FIGURE 11: Kinetics of thermoinactivation of the $NaBH_4$-reduced form of phosphorylase *b* at 53 °C (80 mM Hepes-NaOH, pH 6.8). The dotted and dashed lines correspond to thermal inactivation of the native enzyme. Enzyme concentrations were 1.6 mg/mL (circles and dotted line) and 5.2 mg/mL (squares and dashed line).

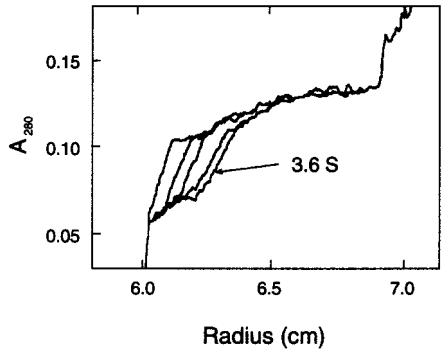

FIGURE 12: Sedimentation velocity pattern vs of $NaBH_4$-reduced form of phosphorylase *b* (0.92 mg/mL) at 53 °C. The rotor speed was 48 000 rpm. The times of sedimentation were 26, 33, 38, 51, and 54 min.

character of the thermal inactivation curves for the reduced phosphorylase *b*, as for the native form, depends on the protein concentration: dilution of the enzyme solution results in acceleration of thermal inactivation. Thus, denaturation of the reduced form of phosphorylase *b* proceeds according to the dissociative mechanism. Second, although the kinetic curve of thermal inactivation of the native enzyme at the concentration 5.2 mg/mL has a well-pronounced lag period, after reduction of the enzyme by sodium borohydride no lag period occurs (Figure 11). The disappearance of lag period on the curves of thermal inactivation for the reduced form of phosphorylase *b* indicates that thermal denaturation of this form does not include the step of predenaturational conformational changes in the dimer. It is known that reduction of phosphorylase *b* by sodium borohydride causes substantial weakening of the intersubunit contacts in the dimer. The reduced phosphorylase *b* can partially dissociate into monomers even at 30 °C at relatively low enzyme concentrations (0.01 mg/mL) (*33*).

Sedimentation analysis of $NaBH_4$-reduced phosphorylase *b* (0.92 mg/mL) at 53 °C (Figure 12) indicates that at sedimentation times used the reduced enzyme form moves as an unfolded monomer ($s_{20,w} = 3.6$ S). Thus, at elevated temperatures $NaBH_4$-reduced phosphorylase *b* dissociates more easily than the native enzyme (cf. Figure 4).

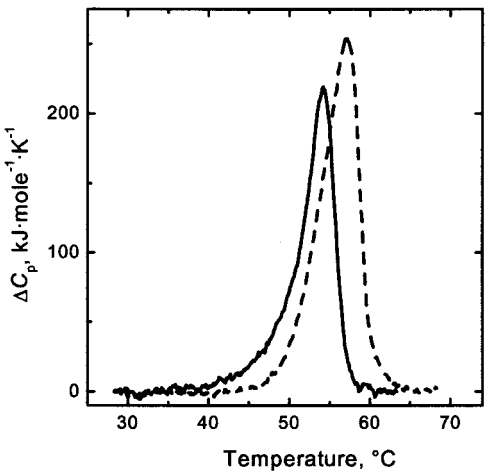

FIGURE 13: Excess heat capacity (ΔC_p) vs temperature profiles for the native (dashed line) and $NaBH_4$-reduced (solid line) forms of phosphorylase *b*. Hepes-KOH, 30 mM, pH 7.0. Enzyme concentration for all the preparations was 1 mg/mL. The scanning rate was 1 °C/min.

The lower stability of sodium borohydride reduced phosphorylase *b*, as compared to the native enzyme, was also supported by DSC data. As seen from Figure 13, the maximum on the ΔC_p vs temperature profile for the reduced form of phosphorylase *b* occurs at 54.2 °C, i.e., at a lower temperature than for the native enzyme (57.0 °C).

DISCUSSION

The distinctive characteristics of the kinetics of thermal inactivation of oligomeric enzymes are the change in the shape of kinetic curves upon variation in the enzyme concentration and the appearance of lag period on the initial part of kinetic curves. The general kinetic scheme of the process of dissociative thermal inactivation of oligomeric enzymes has the following appearance (*10*, *34*).

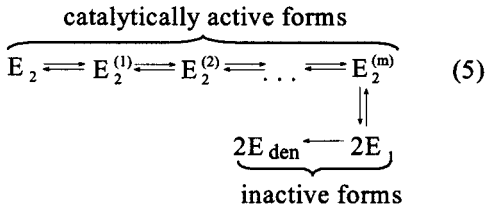

(5)

For the sake of simplicity, we have assumed that the original oligomeric form of the enzyme is a dimer E_2. According to the scheme under discussion, the enzyme oligomer undergoes reversible conformational changes with formation of the enzyme forms $E_2^{(i)}$ ($1 \leq i \leq m$) retaining the catalytic activity. The loss of the enzyme activity is connected with dissociation of the conformationally changed enzyme form $E_2^{(m)}$ into the inactive monomers (E_1) undergoing further denaturation ($E_1 \rightarrow E_{den}$). The denatured monomers usually tend to aggregate, and because of this the process of denaturation becomes irreversible.

Thus, in the scheme under discussion protein denaturation occurs only after the dissociation of the oligomer into the less stable subunits. In turn, the dissociation of the oligomer into subunits is possible only after a series of conformational transitions in the oligomer structure. When explaining the sequence of the conformational changes in the enzyme oligomer, Poltorak et al. (*10*, *34*) postulated that the intersubunit contact in the oligomer consists of discrete subcontacts, disruption of which occurs in a certain order.

In the dimeric molecule of muscle phosphorylase *b*, there are two regions of contact between subunits: one subcontact is located between caps and the other is formed by tower helices of the neighboring subunits (Figure 1). The appearance of lag period on kinetic curves of thermal inactivation of muscle phosphorylase *b* can be explained assuming that the subcontacts differ in stability and their disruption proceeds in a consecutive manner. Thus, the conformationally changed form of the dimer in eq 5 may be the dimer with partially disrupted bonds between subunits. The rupture of one of the subcontacts in the dimeric enzyme facilitates its further dissociation into monomers. The monomers formed undergo irreversible denaturation.

The kinetic scheme of thermal denaturation of muscle phosphorylase *b* proposed by us has the following form:

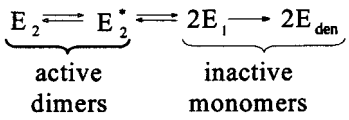

(6)

where E_2 is the native dimeric form of the enzyme and E_2^* is the conformationally changed dimeric form of the enzyme (probably a dimer in which one of the subcontacts is disrupted). The presence of the reversible step of dissociation $E_2^* \rightleftarrows 2E_1$ is supported by the fact that the shape of the kinetic curves of thermoinactivation of phosphorylase *b* is changed with variation of the enzyme concentration, as well as by the data on DSC and analytical ultracentrifugation studies. The presence of reversible pre-denaturation step $E_2 \rightleftarrows E_2^*$ is supported by the fact that the lag period is observed on the thermal inactivation curves.

Equation 2, which does not include the pre-denaturation step has been successfully fitted to DSC profiles obtained at various protein concentration. However, there are some deviations between the experimental and theoretical curves. Probably, these deviations are due to the fact that the model used is simplified. It should be noted, that eq 6 is very complex for fitting: it includes 11 varied parameters instead of 7 for eq 2.

The proposed kinetic scheme of the thermal denaturation of phosphorylase *b* includes the formation of one catalytically active intermediate, namely, the dimeric form E_2^*. In fact, the disruption of contacts between tower helices and caps could proceed stepwise, and therefore formation of several intermediates is possible.

When interpreting the effect of specific ligands on the kinetics of thermoinactivation or reactivation of phosphorylase *b*, we should take into account that the process of denaturation involves the reversible association-dissociation step $D \rightleftarrows 2M$, whereas the reactivation process studied at 30 °C is an irreversible bimolecular reaction $2M \rightarrow D$. The fact that AMP and glucose 6-phosphate are bound in the region of the subunit contact in the dimeric phosphorylase *b* molecule explains the ability of these ligands to interfere with dissociation of the dimer into monomers. One can expect that the monomer is unable to bind AMP or glucose 6-phosphate (or the affinity to these ligands is rather low). That is why the reactivation process is unaffected by AMP

and glucose 6-phosphate. Since the FMN-binding site is located in the cleft between two domains of the subunit, it is likely that the monomeric form retains the affinity to FMN. In this respect, it is worth noting that the apoform of phosphorylase *b*, which exists as a monomer retains the capability for binding of FMN, though the dissociation constant for the apoform−FMN complex is substantially less than the corresponding value for the native enzyme-FMN complex [by a factor of 27 (*21*)]. The stimulating action of FMN on reactivation is probably due to FMN-induced conformational changes in monomers, which favor their association to the dimer.

Phosphorylase *b* cofactor, PLP, is buried in the center of the enzyme molecule at the site, which is situated approximately 1.5 nm from the surface of the enzyme molecule. PLP interacts with the amino acid residues which belong to both domains of the polypeptide chain of the monomer. It is exactly this type of cofactor binding that explains its capability to stabilize the conformation of the native enzyme.

Very noticeable is the fact that the reduction of the aldimine bond between PLP and Lys-680 causes disappearance of the lag period on the kinetic curves of thermoinactivation. This means that in the reduced form of phosphorylase *b* the intersubunit contact is strongly weakened. Therefore, thermal denaturation of the reduced form of phosphorylase *b* follows the simple dissociative mechanism described by eq 2.

Thus, our data show that thermal denaturation of skeletal muscle phosphorylase *b* proceeds according to the dissociative mechanism. The overall mechanism of denaturation involves the stages of predenaturational conformational changes of the dimeric enzyme molecule, dissociation of catalytically active dimers into inactive monomers, and, finally, irreversible denaturation of isolated monomers.

ACKNOWLEDGMENT

We thank Natalia P. Sugrobova for help in experiments with preparation of apophosphorylase *b* and reconstitution of the holoform.

REFERENCES

1. Lin, Y.-Z., Liang, S.-J., Zhou, J.-M., Tsou, C.-L., Wu, P., and Zhou, Z. (1990) *Biochim. Biophys. Acta 1038*, 247−252.
2. Edwards, R. A., Jacobson, A. L., and Huber, R. E. (1990) *Biochemistry 29*, 11001−11008.
3. Chang, B.-S., and Mahoney, R. R. (1994) *Biotechnol. Appl. Biochem. 19*, 169−178.
4. Hernandes-Arana, A., Roio-Dominguez, A., Altamirano, M. M., and Calcagno, M. L. (1993) *Biochemistry 32*, 3644−3648.
5. Consalvi, V., Chiaraluce, R., Politi, L., Pasquo, A., De Rosa, M., and Scandurra, R. (1993) *Biochim. Biophys. Acta 1202*, 207−215.
6. Singh, N., Liu, Z., and Fisher, H. F. (1996) *Biophys. Chem. 63*, 27−36.
7. Qi, X. L., Brownlow, S., Holt, C., and Sellers, P. (1995) *Biochim. Biophys. Acta 1248*, 43−49.
8. Malessa, P. G., and Winter, R. (1999) *Biochemistry 38*, 6512−6519.
9. Afanas'eva G. V., Bulygina, E. R., and Telepneva, V. I. (1995) *Biochemistry (Moscow) 60*, 1082−1088.
10. Poltorak, O. M., Chukhray, E. S., and Torshin, I. Yu. (1998) *Biochemistry (Moscow) 63*, 303−311.
11. Backmann, J., Schafer, G., Wyns, L., and Bonisch, H. (1998) *J. Mol. Biol. 284*, 817−833.
12. Feldmann, K., Zeisel, H., and Helmreich, E. (1972) *Proc. Natl. Acad. Sci. U.S.A. 69*, 2278−2282.
13. Silonova, G. V., and Kurganov, B. I. (1970) *Mol. Biol. (Russian) 4*, 445−459.
14. Huang, C. Y., and Graves, D. J. (1970) *Biochemistry 9*, 660−671.
15. Barford, D., and Johnson, L. N. (1989) *Nature 340*, 609−616.
16. Johnson, L. N., Hajdu, J., Acharya, K. R., Stuart, D. I., McLaughlin, P. L., Oikonomakos, N. G., and Barford, D. (1989) in *Allosteric Enzymes* (Herve, G., Ed.) p 81, CRC Press, Boca Raton, FL.
17. Fischer, E. H., and Krebs, E. G. (1962) *Methods Enzymol. 5*, 368−373.
18. Kastenschmidt, L. L., Kastenschmidt, J., and Helmreich, E. (1968) *Biochemistry 7*, 3590−3607.
19. Sugrobova, N. P., Lissovskaya, N. P., and Kurganov, B. I. (1983) *Biochem. Biophys. Methods 8*, 299−306.
20. Shaltiel, Sh., Hedrick, J. L., and Fisher, E. H. (1966) *Biochemistry 5*, 2108−2117.
21. Chebotareva, N. A., Sugrobova, N. P., Bulanova, L. N., Poznanskaya, A. A., Kurganov B. I., and Gunar, V. I. (1995) *Biochemistry (Moscow) 60*, 1551−1558.
22. Graves, D. J., Sealock, R. W., and Wang, J. H. (1965) *Biochemistry 4*, 290−296.
23. Johnson, G. F., Tu, J. I., Bartlett, M. L. S., and Graves, D. J. (1970) *J. Biol. Chem. 245*, 5560−5568.
24. Hunter, M. J. (1966) *J. Phys. Chem. 70*, 3285−3292.
25. Kornilaev, B. A., Kurganov, B. I., Eronina, T. B., and Livanova, N. B. (1996) *Biochem. Mol. Biol. Int. 38*, 921−927.
26. Arens, E. A., Poltorak, O. M., and Pryakhin, A. N. (1983) *Vestnik Mosk. Univ., Ser. 2 Khimiya (Russian) 22*, 458−462.
27. Chukhray, E. S. (1981) *Vestnik Mosk. Univ., Ser. 2 Khimiya (Russian) 22*, 331−340.
28. Sanchez-Ruiz, J. M. (1992) *Biophys. J. 61*, 921−935.
29. Gunar, V. I., Sugrobova, N. P., Stepanova, S. V., Chebotareva, N. A., Poznanskaja, A. A., and Kurganov, B. I. (1990) in *Enzymes Dependent on Pyridoxal Phosphate and Other Carbonyl Compounds as Cofactors, Proc. of the 8th Intern. Symp. on Vitamin B_6 and Carbonyl Catalysis* (Fukui, T., Kagamiyama, H., Soda, K., and Wada, H., Eds.) p 417.
30. Shachman, H. K. (1959) in *Ultracentrifugation in Biochemistry*, pp 151−157, Academic Press, New York.
31. Bowen, T. J. (1971) *An Introduction to Ultracentrifugation*, Wiley, London.
32. Chukhray, E. S., and Kirsis, V. Kh. (1980) *Vestnik Mosk. Univ., Ser. 2 Khimiya (Russian) 21*, 432−437.
33. DeVincenzi, D. L., and Hedrick, J. L. (1970) *Biochemistry 9*, 2048−2058.
34. Poltorak, O. M., Chukhray, E. S., Tashlitsky, V. N., and Svanidze, R. S. (1980) *Vestnik Mosk. Univ. Ser. 2 Khimiya (Russian) 21*, 224−231.

BI000975W